Dynamic correlations in sliding charge-density waves probed by spatially resolved measurements of voltage oscillations

E. C. Geil and R. E. Thorne
Laboratory of Atomic and Solid State Physics, Cornell University, Ithaca, New York 14853, USA
(Received 16 September 2014; revised manuscript received 4 October 2014; published 4 November 2014)

In sliding charge-density wave (CDW) conductors such as $NbSe_3$, voltage oscillations at a frequency proportional to the local CDW velocity accompany CDW motion and can furnish many insights into the dynamics of these systems. We have used high-performance cryogenic differential amplifiers to make position-dependent measurements of voltage oscillations in the quasisteady state. These measurements yield voltage-voltage and velocity-velocity correlations and the temperature dependence of the CDW's longitudinal and transverse velocity coherence.

DOI: 10.1103/PhysRevB.90.205106 PACS number(s): 71.45.Lr

I. INTRODUCTION

At $T_{p_1} = 145$ K, niobium triselenide ($NbSe_3$) undergoes a Peierls transition to a charge-density wave (CDW) ground state [1], in which the condensed charge number density is given by $n_c = n_0 + \delta n n(\mathbf{Q}\cdot\mathbf{r} + \phi)$, where $\mathbf{Q}$ is the modulation wave vector and $\phi = \phi(\mathbf{r},t)$ is the phase with respect to the atomic lattice.[1] CDWs are pinned by impurities and other defects in the crystal lattice, and the CDW feels a force from each impurity that is periodic (although possibly hysteretic) in the CDW's phase [2]. For applied electric fields E larger than a threshold field E_T, the CDW depins and slides at an average velocity v. Due to phase-dependent interaction with impurities, this motion has an oscillatory component, resulting in coherent voltage oscillations [3] ("narrow-band noise") at a "washboard" frequency

$$f = \frac{1}{2\pi}\frac{\partial\phi}{\partial t} = \frac{Q}{2\pi}v = \frac{v}{\lambda}, \tag{1}$$

where $\lambda = 1.43$ nm is the CDW wavelength.

These voltage oscillations provide perhaps the most direct experimental probe of the CDW's sliding motion. Velocity-coherent motion produces voltage spectra with sharp, single peaks. However, if the velocity is spatially inhomogeneous or exhibits nonperiodic fluctuations, the spectral peaks are broadened or split. Inhomogeneous, fluctuating CDW motion is also accompanied by low-frequency "broadband" noise (BBN) with a $1/f^{\alpha}$ spectral distribution [3–5].

Previous electrical transport studies of CDW conduction "noise" largely fall into two broad categories. In the first, the voltage is measured in a two-probe configuration, or in a four-probe configuration with strongly perturbing (i.e., current shunting and phase-slip inducing) voltage contacts [3,6–10]. Such measurements provide no spatial information, and it is difficult to disentangle bulk behavior from behavior associated with phase slip near contacts [11–14].

In the second measurement category, voltage contacts are placed at multiple locations along the length of the sample, and the voltage across two or more contact pairs is measured [13,15–21]. This enables observation of the spatial variation of CDW dynamics, and of voltage-voltage correlations between different contact pairs [21]. However, for voltage contacts to be weakly or nonperturbing of the CDW's deformations and motion, they must be narrow ($\lesssim 10$ μm) and thin [14,22,23]. The large impedances of these contacts combine with cryostat wiring capacitances to limit measurement bandwidths to $\sim$1 MHz. As a result, voltage oscillations at the washboard frequency f—which directly give the CDW velocity—can only be probed within this bandwidth, which is typically exceeded at biases beyond approximately $1.2E_T$. Noise and interference introduced by routing signals to room-temperature amplifiers can also limit measurement sensitivity. Spatially resolved measurements of time-varying voltages using nonperturbing contacts have thus largely been limited to the study of transients [13], broadband noise [21], and low-frequency fluctuators [17–20].

To overcome these challenges, we have designed and constructed high-performance cryogenic differential amplifiers, and used these with arrays of voltage contacts to measure voltage oscillations at the washboard frequency in $NbSe_3$ crystals. These wide-bandwidth, spatially resolved measurements reveal several aspects of the CDW's dynamical coherence and correlations, and illuminate the roles of bulk, shear, and contact plasticity. Application of these amplifiers in the study of transient CDW dynamics is described elsewhere [24].

II. METHODS

High-purity $NbSe_3$ crystals were grown according to the procedures in Ref. [25]. Step-free, optically uniform crystals were selected, laid atop arrays of 20-nm high gold contact pads on alumina substrates, and secured with a thin film of ethyl cellulose. Voltage contacts were all 2-μm wide; contacts of this width have been shown to be nonperturbing in $NbSe_3$ at temperatures up to 130 K [14]. Current contacts were at least 100-μm wide to minimize contact resistances and, together with the high-thermal conductivity substrate, minimized sample heating.

The voltages between pairs of contacts were amplified by high-performance dc-coupled cryogenic differential amplifiers. The design is similar to that described in Ref. [26]. The cryogenic input stage comprises a differential pair of NESG3031 SiGe transistors with input bias currents of less than 30-nA, which are buffered (in a cascode topology)

[1] $NbSe_3$ undergoes a second, independent CDW transition at $T_{p_2} = 59$K. This CDW exhibits similar transport properties and is not studied here.

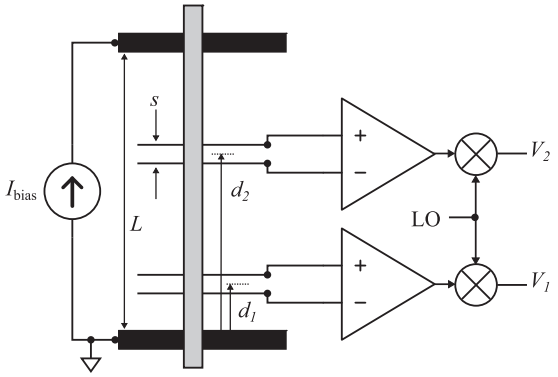

FIG. 1. Sample contacts, differential amplifiers, and RF mixers used for measurements of voltage oscillations in $NbSe_3$. L is the spacing between current contacts, s is spacing between voltage contacts within a contact pair, and d_i is distance from the reference current contact to the center of the ith voltage contact pair. For measurements of fluctuations of the coherent voltage oscillation frequency, the signal from each voltage contact pair was heterodyned using an LO signal to a fixed and much lower intermediate frequency, and bandpass filtered to remove harmonics introduced by the mixing.

by OPA836 SiGe op-amps. A room-temperature differential to single-ended stage further improves the common-mode rejection ratio (CMRR) and voltage gain. The system achieves an overall gain of 300 V/V over a 60-MHz −3-dB bandwidth, a CMRR of −90 dB, and a noise floor of 0.9 nV $Hz^{-\frac{1}{2}}$ at 77 K (the cryogenic stage's temperature during measurements). More details are given elsewhere [27]. Two complete amplifiers were used to amplify the differential voltage between two pairs of contacts. The amplifier outputs were recorded using a LeCroy Waverunner 44 Xi digital oscilloscope.

Measurements of the coherent voltage oscillations over long time intervals—useful for studying their fluctuations—present a particular challenge. For example, tracking a 50 MHz peak requires a sampling rate of at least 100 MHz (and much larger if the many harmonics of the fundamental peak are not to be aliased). With typical acquisition times per measurement of order one second and hundreds or thousands of measurements per sample, managing the data generated would require significant effort.

To address this challenge, for measurements of fluctuations of the coherent voltage oscillations and their spatial correlations, we used an RF mixer to heterodyne the oscillations down to a lower beat frequency. A local oscillator was tuned to a frequency approximately 300 kHz below that of the voltage oscillation's fundamental spectral peak, mixed with the output from the differential amplifiers, and then the heterodyned signal was low-pass filtered to remove harmonics. For the highly coherent samples used here, the spectral peak quality factors were on the order of at least several hundred, so even at $f_{NBN} =$ 50 MHz, the peaks fit easily into a 1-MHz digitizer bandwidth. The amplifier and mixer circuits are shown in Fig. 1.

III. RESULTS

Approximately 30 $NbSe_3$ crystals were examined for suitable spectral coherence of their voltage oscillations and for completeness of their mode locking to an applied ac voltage. Of these, six were used in an initial exploration of spatio-temporal correlations. Data are presented here for three samples, denoted sample 1, 2, and 3, which had the most coherent response. Table I gives the dimensions of these samples.

TABLE I. Dimensions of the three $NbSe_3$ samples for which data are reported. The length and width were determined optically, and the thickness was determined from these dimensions, the $T =$ 300 K sample resistance, and the known $NbSe_3$ resistivity of 1.85×10^{-6} Ωm [29].

No.	Length (μm)	Width (μm)	Thickness (μm)
1	3000	72	0.43
2	1000	9	0.36
3	1000	29	0.32

A. Spectral coherence versus temperature

Sample 1 showed an exceptionally coherent response in the mid-sample region (far from the region of phase slip near current contacts [13,14] at temperatures between 80 and 110 K. At these temperatures, the voltage spectrum had a single, sharp peak (plus harmonics); the measured peak width was limited by the Fourier transform resolution, but the quality factor was at least 1000. The sample also showed complete mode locking to an applied ac voltage (as measured at 120 K, 15-MHz RF frequency).

However, as the temperature was raised from 110 K to just below T_{P_1}, the CDW in Sample 1 appeared to break up into progressively smaller regions with somewhat different peak frequencies. Figure 2 shows the power spectral density versus temperature of the voltages recorded at two contact pairs for a fixed bias current of 6.5 mA. The spectra were continuously recorded as the sample was warmed from 80 to 142 K at a rate of 0.5 K/min; spectra recorded on cooling through the same temperature range showed the same behavior. The lower panel of Fig. 2 shows a closer view of the high-temperature region where the moving CDW "melts." There is a loss of spectral coherence not only between the contact pairs (separated by 900 μm), visible as a splitting between the blue and orange traces, but also within the region of the CDW observed by each contact pair (approximately 50 μm long by 72 μm wide), visible as a splitting of the blue and orange traces themselves. Qualitatively similar melting behavior was observed in all six samples for which this measurement was performed, although the detailed pattern depended on sample perfection. The fine details of the spectral structure in Fig. 2 were made visible by the exceptionally low noise floor obtained using our cryogenic amplifier, which was typically two orders of magnitude below the baseline noise level generated by the sample.

The data in Fig. 2 were acquired from contact pairs far (1000 and 1100 μm) from the current contacts, where phase slip from current conversion is less significant [13,14,28]. Figure 3 shows spectra from sample 2 ($L = 1$ mm) acquired using two contact pairs located 75 and 500 μm, respectively, from the negative current contact (from which the negatively charged CDW slides toward the positive contact). This sample, too,

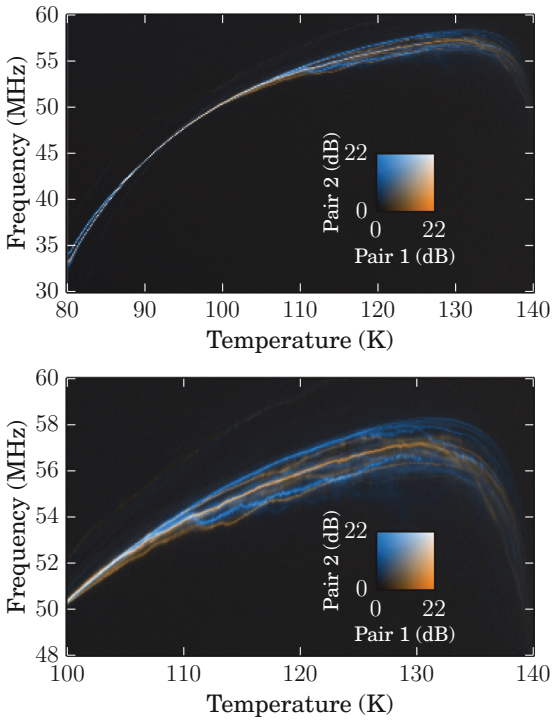

FIG. 2. (Color online) (Top) Power spectral density (indicated by the color scheme in the inset) vs frequency and temperature for Sample 1 ($L = 3000$ μm), measured in response to a constant current bias of $I = +6.5$ mA. Spectra were recorded at pair 1 (orange) located at $d_1 = 1000$ μm from the negative current contact, and pair 2 (blue) located at $d_2 = 1900$ μm. Both pairs had a contact spacing of 50 μm, and were far from the region near the current contacts (at $d = 0$ and 3000 μm) where CDW to single-particle current conversion occurs. Bottom: An expanded view of the high-temperature region. Data acquired with fixed oscillation peak frequency rather than fixed bias current are given in Ref. [34].

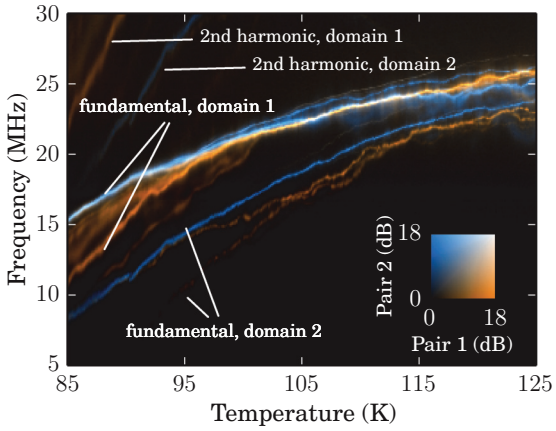

FIG. 3. (Color online) Power spectral density (indicated by the color scheme in the inset) vs frequency and temperature for sample 2 ($L = 1000$ μm), measured in response to a constant current bias $I = +250$ mA. Spectra were recorded at pair 1 (orange) located at $d_1 = 75$ μm from the negative current contact, and pair 2 (blue) located at $d_2 = 500$ μm, near the sample's midpoint. Both pairs had a contact spacing of 50 μm. Sample 2 had a thickness step near one edge, running along its length, dividing the crystal into two domains with different pinning strengths. The CDW velocity is smaller in the thinner, more strongly pinned domain 2 than in domain 1. Harmonics of the fundamental spectral peaks from both domains are visible in the upper left. Data acquired with fixed oscillation peak frequency and fixed E/E_T rather than fixed bias current are given in Ref. [34].

mode-locked completely (at 120 K, RF frequency 15 MHz), but had a small thickness step close to one edge and running along its length. This step defined two crystal domains of different thicknesses and thus different pinning strengths [29], and resulted in velocity shear between the two domains [5]. The thinner, smaller domain 2 generated spectral peaks at lower frequencies and with roughly 4% of the power compared to those of domain 1.

The main feature of interest in Fig. 3 is that in the vicinity of the current contact, the fundamental peak of Domain 1 shows increasing splitting as the temperature drops below 98 K. One component of the spectral peak remains coherent with the peak from the midsample contact pair, and the other broadens and sharply decreases in mean frequency. This behavior was asymmetric with respect to the current direction: spectra acquired with the current direction reversed showed little splitting in the vicinity of the current contact below 98 K. Consistent with the present observations, previous spatially resolved current-voltage measurements revealed a decay of the average CDW current within a voltage contact pair as each current contact was approached, and a much larger length scale for this decay near the negative contact than near the positive contact [14]; spatially resolved x-ray diffraction measurements of the longitudinal CDW strain (associated with boundary conditions at current contacts) in $NbSe_3$ showed a similar length scale and asymmetry [28]. However, the full velocity spectra in Fig. 3 show that the velocity does not decay smoothly. Instead, the presence of discrete spectral peaks suggests that as the current contact is approached, the sample segments into regions of nearly constant but decreasing velocity, with large phase slip rates between these regions producing the velocity differences. A similar breakup of the CDW into velocity coherent domains with different mean velocities has been observed in response to temperature gradients applied along the length of $NbSe_3$ crystals [30].

B. Velocity fluctuations at a single contact pair

In all samples studied, the frequency of the voltage oscillation peaks fluctuated with time. These fluctuations were most apparent for highly coherent samples with narrow spectral peaks. Using the heterodyne technique described in Sec. II, voltage oscillations were recorded for 200 intervals of 1 s. Approximately 12 s were required between successive intervals to transfer data from the oscilloscope, so the total elapsed time was ~2600 s. For each segment, the spectrogram of the signal was computed, and the peak frequency $f_p(t)$ found at 0.8-ms intervals. The power spectrum of the peak frequencies (a type of "second spectrum" [31]) was then computed. This procedure allowed the frequency dependence of the fluctuation amplitude to be measured over five decades of frequency.

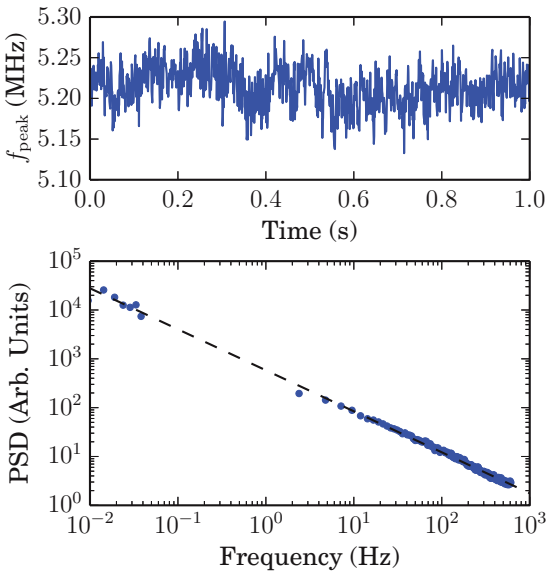

FIG. 4. (Color online) (Top) Fluctuations of the peak frequency of the CDW's "washboard" voltage oscillations for sample 2 at $T = 80$ K and with a bias current $I = 1.5I_T$. The peak width was approximately 30 kHz. The voltage contacts were located at the sample midpoint (500 μm from the nearest current contact). The measured voltage was heterodyned using an LO frequency of 4.9 MHz to a mean IF of 500 kHz, and then low-pass filtered with a 1-MHz bandwidth. Bottom: Power spectral density of the fluctuations of the peak frequency. The dashed line indicates a fit $S(f) \sim f^{-\alpha}$ with $\alpha = 0.84$. The gap in the data is due to the time delay between measurement intervals during which data was transferred from the oscilloscope.

Figure 4 shows typical spectrogram peak frequency versus time data for a single one second interval, and the power spectrum of the peak frequency fluctuations determined from 200 such intervals. The data were obtained from sample 2 at $T =$ 80 K, using a voltage contact pair at $d = 500$ μm, near the middle of the sample. The power spectrum shows power-law behavior over five decades in frequency. The dashed line shows a fit $S(f) \sim f^{-\alpha}$ with $\alpha = 0.84$. Similar values of the exponent were obtained at all temperatures examined. This exponent is comparable to values of 0.8–1.1 measured previously for the power spectrum of the low-frequency (<100 kHz) noise that accompanies CDW motion in $NbSe_3$ [4,5]. Low-frequency (broadband) noise has been attributed to CDW phase slip, with the largest contribution arising from CDW shear along transverse thickness steps [5], and other contributions from slip near current contacts and near other crystal defects that create CDW velocity discontinuities. Fluctuations in the peak frequency and spectral shape of the coherent voltage oscillations likely arise from the same mechanisms.

C. Velocity fluctuation correlations between contact pairs

Spatial correlations of the CDW velocity fluctuations were measured by concurrently recording voltage oscillations between two pairs of contacts probing different segments of the sample, using the configuration shown in Fig. 1. Voltage oscillations were heterodyned and digitized in 100 one second intervals, spectrograms were computed, and peak frequencies versus time identified as above. The equal-time correlation coefficient between frequency fluctuations in two sample segments was then computed as

$$r^2 = \frac{\langle [(f_1 - \overline{f_1})(f_2 - \overline{f_2})) \rangle}{\sigma_{f_1}\sigma_{f_2}}, \tag{2}$$

where f_1 and f_2 are the frequencies at pair 1 and pair 2 (computed as the centroid of the peak in the power spectral density), $\langle\cdot\rangle$ is a time average, and σ_{f_i} is the standard deviation.

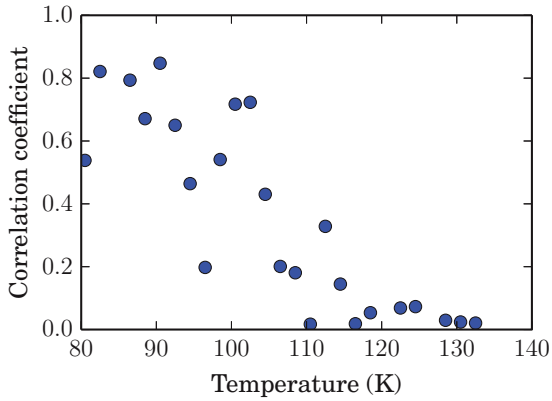

FIG. 5. (Color online) Correlation coefficient vs temperature for the fluctuations of the washboard peak frequency between two contact pairs separated by 400 μm, for sample 2. The bias current was adjusted to maintain the NBN peak frequency at 5.6 MHz.

Figure 5 shows the correlation coefficient versus temperature from 80 to 130 K for sample 2, dc-biased to a mean washboard oscillation peak frequency of 5.6 MHz. The separation between the two contact pairs was 400 μm, and the smallest voltage contact–current contact distance was 100 μm. There is a large amount of scatter, but the general trend is from nearly perfect correlation at 80 K to zero correlation above 130 K. All of the roughly half-dozen samples studied showed a relatively sharp drop in correlation in the vicinity of 100 K. This temperature roughly corresponds with the temperature above which significant broadening and splitting of the coherent oscillation spectra is observed in Fig. 2. Both effects likely result from increased bulk CDW phase slip/plasticity, arising from the decrease in CDW order parameter, elastic rigidity, and barriers for phase slip as $T \to T_{p_1}$, and from increased thermal energy available for activated phase slip processes.

Another measure of spatial correlations between velocity fluctuations is the spectral coherence, in general, defined as

$$C_{x_1x_2}(f) = \frac{\left|S_{x_1x_2}(f)\right|^2}{S_{x_1x_1}(f)S_{x_2x_2}(f)}, \tag{3}$$

where $S_{x_1x_2}(f)$ is the cross-spectral density, and $S_{x_1x_1}(f)$ and $S_{x_2x_2}(f)$ are the autospectral densities of signals x_1 and x_2, respectively. The coherence satisfies $0 \leqslant C_{x_1x_2} \leqslant 1$, with $C_{x_1x_2} = 1$ indicating perfect coherence. In the present case, the signals x_1 and x_2 are the peak frequencies $f_{\rm peak}(t)$ extracted from spectrograms as in Fig. 4 for two different contact pairs, and the frequency f is that of the fluctuations in the peak frequencies (and thus in CDW velocities).

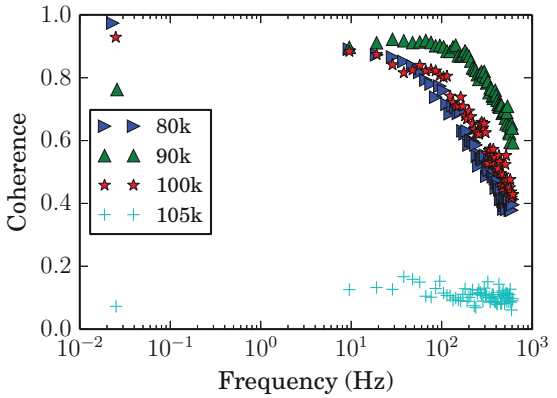

FIG. 6. (Color online) Coherence of washboard frequency fluctuations in sample 2 for two contact pairs separated by 400 μm, located a minimum of 100 μm from the current contacts. The bias current was adjusted to maintain the NBN peak frequency at 5.6 MHz.

Figure 6 shows the coherence versus fluctuation frequency f for sample 2 at several temperatures, evaluated using voltages measured at the same contact pairs as in Fig. 2 and for a fixed peak coherent oscillation frequency of 5.6 MHz. At temperatures below ~100 K, the coherence is nearly perfect for fluctuation frequencies at below ~100 Hz, and then drops off rapidly at higher frequencies. This indicates that the low-frequency variations in peak frequency are strongly correlated over the 400-μm separation between contact pairs, but that frequency fluctuations beyond ~1 kHz, or roughly 0.02% of the peak frequency, are largely uncorrelated.

D. Voltage-voltage correlations

In addition to frequency-frequency (velocity-velocity) correlations, direct voltage-voltage correlations between different sample segments can be evaluated. The normalized cross-correlation is given by

$$C_{\Delta t}[v_1, v_2] = \frac{\langle v_1(t+\Delta t)v_2(t)\rangle - \langle v_1\rangle\langle v_2\rangle}{\sqrt{\langle v_1^2\rangle - \langle v_1\rangle^2}\sqrt{\langle v_2^2\rangle - \langle v_2\rangle^2}}, \qquad (4)$$

where $v_1(t)$ and $v_2(t)$ are voltages at two contact pairs, and $\langle\cdot\rangle$ denotes a time average. Previous work [21] examined voltage-voltage correlations at low frequencies ($f < 10$ kHz) in $NbSe_3$ at $T = 70$ K. The equal-time correlation coefficient was zero for fields below the depinning threshold, rose steeply to a maximum just above threshold, and then decayed at larger biases. We have extended these studies to higher frequencies and to temperatures between 80 and 130 K.

Voltage oscillations were measured directly, without heterodyning, from samples 1 and 3. Figure 7 shows the equal-time voltage-voltage correlation between contact pairs separated by 50 μm, as a function of bias field and measurement bandwidth at $T = 90$ and 120 K, for sample 3. The general variation with bias is consistent with that reported in Ref. [21]. The maximum correlation coefficient observed above threshold decreases with increasing measurement bandwidth, and also with increasing temperature. For larger measurement bandwidths, the voltage fluctuations become dominated by uncorrelated high-frequency components generated by CDW motion. This

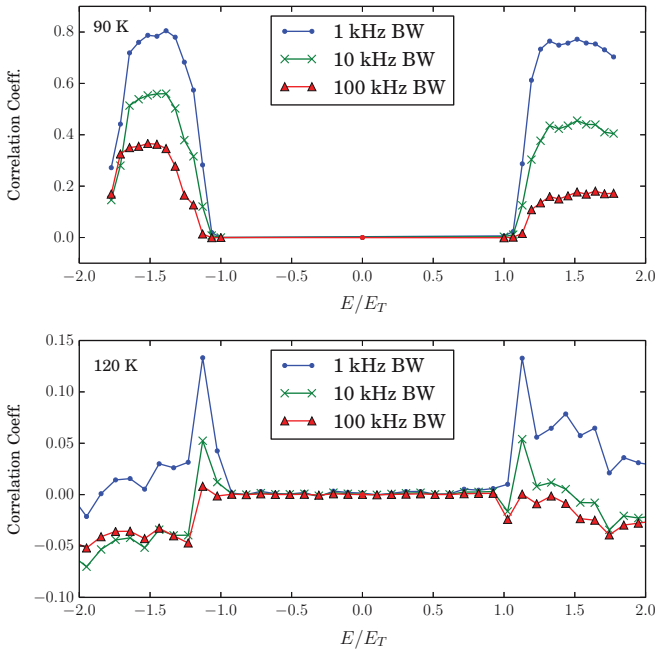

FIG. 7. (Color online) Equal-time correlation coefficient C_0 of voltage oscillations in sample 3, measured at contact pairs separated by 50 μm and located in the middle third of the sample, as a function of bias E/E_T and measurement bandwidth.

can be seen by computing the spectral coherence between voltages measured at two contact pairs, which drops off sharply above ~1 kHz.

As the measurement bandwidth increases into the MHz range, the equal time correlation coefficient C_0 drops to near zero. However, high-quality samples do exhibit weak long-range voltage correlations associated with oscillations near the washboard frequency. Figure 8 shows the equal-time voltage correlation coefficient versus temperature measured

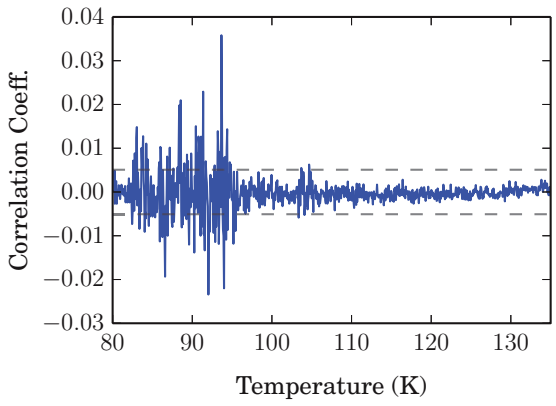

FIG. 8. (Color online) Equal-time correlation coefficient C_0, over a 60-MHz bandwidth, of voltage oscillations in sample 1, measured at contact pairs separated by 900 μm and located in the middle third of the sample. The sample bias current was adjusted to maintain a NBN peak frequency of 49 MHz as the temperature was increased at a rate of 0.3 K/min. The dashed lines are 90% significance levels for a nonzero C_0, as estimated via a bootstrapping procedure. A negative coefficient indicates a phase reversal.

using contact pairs at least 1 mm from the current contacts of sample 1, evaluated using the full amplifier (−3 dB) bandwidth of 60 MHz. The separation between the two contact pairs was 900 μm, and the sample bias current was adjusted to maintain a NBN peak frequency of 49 MHz at all temperatures. To improve estimates of the small correlation coefficients, averages were taken over multiple successive traces; these also permitted bootstrap estimates of confidence intervals for a null correlation coefficient (by calculating correlations between traces acquired at different times). Figure 8 shows that small but significant correlations appear sporadically at temperatures below 100 K. These could indicate intermittent long-range locking or synchronization between CDW regions.

IV. CONCLUSIONS

The present measurements of CDW velocity and voltage fluctuations and their spatial correlations are consistent with the following picture of the temperature-dependent coherence properties of the T_{p_1} CDW in $NbSe_3$. At low temperatures ($\lesssim$90 K), the phase slip required for conversion between single-particle and collective currents extends to substantial distances from the current contacts. The CDW velocity and phase-slip rate do not vary smoothly with the position near contacts. Instead, the CDW tends to break up into velocity-coherent domains, between which the phase slip is concentrated. Previous studies have shown that crystal defects can cause CDW velocity discontinuities and phase slip far from the current contacts; the sample-dependent spectral structure observed here suggests that crystal defects may play a role in concentrating the slip that occurs near the current contacts as well.

As the temperature increases, the region of phase slip shrinks toward the current contacts. In high-quality samples at temperatures between ∼90 and ∼105 K, the CDW slides uniformly over nearly the entire sample length.

At still higher temperatures, the CDW's shear and longitudinal elastic strengths decrease, and thermally initiated phase slip including at sample defects becomes easier. The CDW breaks up into longitudinal and shear domains. The size of these velocity-coherent domains decreases, and their number increases, until the CDW melts completely at the transition temperature.

The wide-bandwidth, high-performance cryogenic amplifiers used here allow unprecedented access to the CDW's velocity and its fluctuations. The present measurements were limited in spatial resolution by the 50-μm spacing of voltage contacts within each pair, and also by crystal widths of 9 to 72 μm. The CDW's dynamics within such large volumes, containing perhaps 10^3 phase correlation volumes and possibly also large numbers of phase slip centers/CDW dislocations are thus quite complicated. However, substrates with many more finely-spaced contacts can be fabricated, narrower and thinner crystals can be used, and the crystals themselves can be micro- and nanofabricated to isolate and/or probe much smaller volumes [23,32,33]. Provided that contact resistances are maintained below ∼10 kΩ, measurement bandwidths of at least 10 MHz, sufficient for robust measurements of coherent oscillations and CDW velocity fluctuations to biases well above E_T, should be achievable. This approach should facilitate a rich array of experiments that will more directly probe microscopic aspects of CDW dynamics.

ACKNOWLEDGMENTS

This work was supported by the National Science Foundation (Grant DMR-0805240). Substrates were fabricated at the Cornell NanoScale Facility, a member of the National Nanotechnology Infrastructure Network, which is supported by the National Science Foundation (Grant ECCS-0335765).

[1] P. Monceau, Adv. Phys. **61**, 325 (2012).
[2] I. Tutto and A. Zawadowski, Phys. Rev. B **32**, 2449 (1985).
[3] R. M. Fleming and C. C. Grimes, Phys. Rev. Lett. **42**, 1423 (1979).
[4] J. Richard, P. Monceau, M. Papoular, and M. Renard, J. Phys. C **15**, 7157 (1982).
[5] M. P. Maher, T. L. Adelman, J. McCarten, D. Dicarlo, and R. E. Thorne, Phys. Rev. B **43**, 9968 (1991).
[6] M. Weger, G. Grüner, and W. G. Clark, Solid State Comm. **44**, 1179 (1982).
[7] J. Richard, P. Monceau, and M. Renard, Phys. Rev. B **25**, 948 (1982).
[8] S. Bhattacharya, J. P. Stokes, M. O. Robbins, and R. A. Klemm, Phys. Rev. Lett. **54**, 2453 (1985).
[9] S. Bhattacharya, J. P. Stokes, M. J. Higgins, and R. A. Klemm, Phys. Rev. Lett. **59**, 1849 (1987).
[10] R. E. Thorne, W. G. Lyons, J. W. Lyding, J. R. Tucker, and J. Bardeen, Phys. Rev. B **35**, 6348 (1987).
[11] N. P. Ong and G. Verma, Phys. Rev. B **27**, 4495 (1983).
[12] J. C. Gill, J. Phys. C **19**, 6589 (1986).
[13] T. L. Adelman, M. C. de Lind van Wijngaarden, S. V. Zaitsev-Zotov, D. DiCarlo, and R. E. Thorne, Phys. Rev. B **53**, 1833 (1996).
[14] S. G. Lemay, M. C. de Lind van Wijngaarden, T. L. Adelman, and R. E. Thorne, Phys. Rev. B **57**, 12781 (1998).
[15] S. E. Brown and L. Mihaly, Phys. Rev. Lett. **55**, 742 (1985).
[16] P. Monceau, M. Renard, J. Richard, and M. C. Saint-Lager, Physica B **143**, 64 (1986).
[17] I. Bloom, A. C. Marley, and M. B. Weissman, Phys. Rev. Lett. **71**, 4385 (1993).
[18] I. Bloom, A. C. Marley, and M. B. Weissman, Phys. Rev. B **50**, 12218 (1994).
[19] I. Bloom, A. C. Marley, and M. B. Weissman, Phys. Rev. B **50**, 5081 (1994).
[20] A. C. Marley, M. B. Weissman, and H. T. Hardner, Phys. Rev. B **50**, 4878 (1994).

[21] S. G. Lemay, K. Cicak, K. O'Neill, and R. E. Thorne, Phys. Rev. B **64**, 205106 (2001).
[22] M. P. Maher, T. L. Adelman, D. A. Dicarlo, J. P. McCarten and R. E. Thorne, Phys. Rev. B **52**, 13850 (1995).
[23] E. Slot and H. S. J. van der Zant, J. Phys. IV France **12**, Pr9-103 (2002).
[24] E. C. Geil and R. E. Thorne, Phys. Rev. Lett. (to be published).
[25] R. E. Thorne, Phys. Rev. B **45**, 5804 (1992).
[26] N. Beev and M. Kiviranta, Cryogenics **57**, 129 (2013).
[27] E. C. Geil, Ph.D. thesis, Cornell University, 2014.
[28] S. Brazovskii, N. Kirova, H. Requardt, F. Ya. Nad, P. Monceau, R. Currat, J. E. Lorenzo, G. Grubel, and Ch. Vettier, Phys. Rev. B **61**, 10640 (2000).
[29] J. McCarten, D. A. DiCarlo, M. P. Maher, T. L. Adelman, and R. E. Thorne, Phys. Rev. B **46**, 4456 (1992).
[30] J. W. Lyding, J. S. Hubacek, G. Gammie, and R. E. Thorne, Phys. Rev. B **33**, 4341 (1986).
[31] M. B. Weissman, Annu. Rev. Mater. Sci. **26**, 395 (1996).
[32] O. C. Mantel, F. Chalin, C. Dekker, and H. S. J. van der Zant, Phys. Rev. Lett. **84**, 538 (2000).
[33] A. F. Isakovic, K. Cicak, and R. E. Thorne, Phys. Rev. B **77**, 115141 (2008).
[34] See Supplemental Material at http://link.aps.org/supplemental/10.1103/PhysRevB.90.205106 for measurements as in Figs. 2 and 3 but with fixed peak washboard oscillation frequency instead of fixed current.